

ANALYSIS OF THE DYNAMIC BEHAVIOUR OF 10MW BOTTOM-FIXED OFFSHORE WIND TURBINES

Y. Yang *University of Shanghai for Science and Technology, P. R. China; Liverpool John Moores University, UK;*

M. Bashir *Liverpool John Moores University, UK;*

C. Li *University of Shanghai for Science and Technology, P. R. China;*

J. Wang & S. Loughney *Liverpool John Moores University, UK;*

ABSTRACT

This paper presents a comparative study of the dynamic responses of 10 MW offshore wind turbines supported by a monopile and tripod. The baseline tower of the original land-based wind turbine has been scaled to meet the structural strength requirements for application in water depth of 50m. The open source numerical analysis tool, FAST (Fatigue, Aerodynamic, Structural, Turbulent), is used to conduct the fully coupled simulations. The modal analysis of the wind turbines associated with the two types of support structures is performed using a finite element analysis software suite, ABAQUS and the FAST tool. The results show good agreements between the FAST and ABAQUS responses, indicating that FAST can be used to accurately perform dynamic analysis for the 10 MW wind turbine. The Eigen-frequencies of the 1st eigenmodes of the tripod support structure fall within the blade pass frequency (3P) range, resulting in larger fluctuation ranges of the responses compared to the monopile type. The tripod support structure requires further improvements to avoid the structural natural frequencies coinciding with the 3P frequency in operational speed range of the wind turbine. The rotational frequency (1P) contributes significantly to the blade-tip deflections. The edgewise mode has been activated, while the flapwise mode is invisible. The results presented in this study can potentially contribute to the improvements in the design of support structures of large wind turbines.

1. INTRODUCTION

In the past decade, the development of offshore wind energy has received much attention. The 2017 Global Wind Energy Council's (GWEC) annual wind report stated that the offshore segment had a record year with 4,334 MW of installations, an 87% increase on the 2016 market [1]. Currently, the majority type of Offshore Wind Turbines (OWTs) is bottom-fixed due to cost and technological limitations. Monopile and tripod support structures have been widely applied in shallow and transitional water areas. According to the statistics of European Wind Energy Association (EWEA) [2], around 90% OWTs in European water are supported on monopiles and tripods. The rated power capacities of the installed wind turbines fall within the range of 1.5 MW to 5 MW. It is imperative to develop larger wind turbines with rated power capacities in the order of 8 MW to 10 MW for the reduction of the installation and maintenance costs of offshore wind farms.

Technical University of Denmark (DTU) in collaboration with Vestas carried out a design of 10 MW rotor and its corresponding land-based tower for the Light Rotor project [3]. The DTU 10 MW wind turbine concept requires larger support structures for offshore applications. Velarde et al. [4-5] proposed four monopile concepts for the DTU 10 MW wind turbine installed in different water depths, namely, 20m, 30m, 40m and 50m. The proposed concepts were obtained through modifications of baseline tower in accordance with the appropriate scaling factors in order to enhance the structural strength and other offshore installation and operational considerations. In developing the monopile models, the nonlinear soil-structure interaction was modelled as distributed springs. The stiffness of the soil springs was derived by using a numerical tool, Plaxis 3D. For comparison purposes, the method recommended by the American Petroleum Institute (API) [6] was employed to obtain the nonlinear stiffness of each soil spring. The ultimate limit state analysis for the monopiles was carried out using RIFLEX by ignoring the coupled effects of wind and wave. In another sample of the application of the DTU 10 MW wind turbine, the

INNWIND.EU project proposed the use of three jackets for wind turbine foundations in 50m water areas. The fatigue and ultimate limit state analysis was performed for each of the jackets in the INNWIND project. However, the deliverables for the project are more focused on the development of the support structures without considering the coupled effects of wind and wave. Although several studies have conducted and presented work on the dynamic analysis of offshore wind turbines by considering wind and wave parameters, with the rated power capacities of the investigated wind turbines limited to 5 MW [7-15]. Due to the more flexible nature of blades and support structures of the 10 MW wind turbine compared to 5 MW wind turbines, the results of studies on 5 MW wind turbines cannot be applied directly to the 10 MW ones.

Therefore, this study focuses on the coupled analysis of 10 MW offshore bottom-fixed wind turbines. The monopile developed in [4] for 50m water depth is adopted for this study. Moreover, in order to present a comparative study on the difference between the support structures, a tripod is also developed through scaling the tripod applied for the NREL 5 MW wind turbine [16]. In this study, an open source numerical analysis tool, FAST, is used to conduct the simulations. The aero-hydro-elastic coupling model of the wind turbine has been established. Blade Element Momentum Theory (BEMT) and Dynamic Wake Model (DWM) are applied to conduct the calculations regarding the aerodynamic loads acting on the rotor and tower. The hydrodynamic loads on the support structures are calculated using the Morison equations based on the wave speed and acceleration data generated through Airy wave theory and JONSWAP spectrum. The structural dynamic model of the support structure is established using Finite Element Method (FEM) based on Timoshenko beam theory. The Craig-Bampton method [17] is employed to reduce the degrees of freedom for a more efficient solution. Comparisons of the dynamic responses of the wind turbines on monopile and tripod substructures are presented. This research can potentially contribute to improvements in the design of support structures of large wind turbines located in transitional waters.

2. DESCRIPTION OF THE REFERENCE WIND TURBINES

The reference 10 MW wind turbine, developed by DTU Wind Energy and Vestas for the Light Rotor project, is used in this study. The three-bladed wind turbine has been classed as an IEC class 1A wind climate. The rated power is 10 MW and the rated wind speed is 11.4 m/s. Further details on the development of the rotor are described in [3]. The original tower was designed for the land-based type. However, in order to meet the structural strength requirements of offshore wind turbines installed in 50m water depth areas, the diameter and thickness of the tower are scaled with factors of 1.25 and 1.5, respectively [4]. The modified tower diameters at top and base are 7 m and 10.5 m, and the thicknesses at top and base are 30 mm and 57 mm.

In this study, two bottom-fixed support structures are used for comparisons as visualized in Figure 1. The monopile was developed by Velarde [4]. On the basis of the tripod structure proposed for the NREL 5MW wind turbine in the phase III of the Offshore Code Comparison Collaboration (OC3) project [16], this study presents a new tripod structure for the DTU 10 MW reference wind turbine. The masses of the monopile and tripod support structures are 2.08×10^7 kg and 1.13×10^8 kg, respectively. Table 1 presents the main specifications of the DTU 10 MW reference wind turbine with the scaled tower.

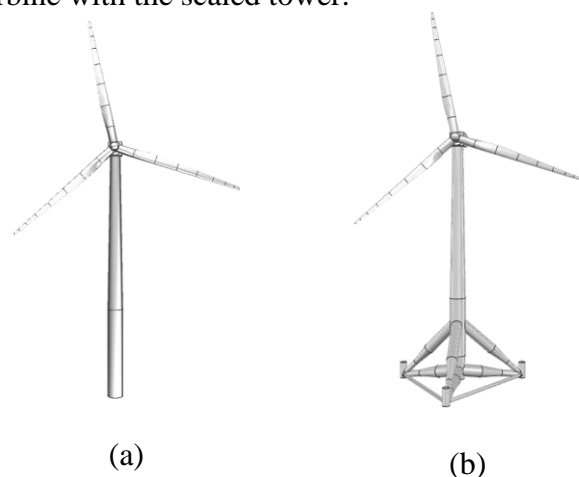


Figure 1: The DTU 10MW wind turbines supported by: (a) the monopile and (b) the tripod.

Table 1: Main specifications of the tower-scaled DTU 10 MW reference wind turbine

Property (Unit)	Value
Rated power (MW)	10.0
Rated wind speed (m/s)	11.4
Cut-in speed (m/s)	4.0
Cut-out speed (m/s)	25.0
Rated rotor speed (rpm)	9.6
Rotor diameter (m)	178.3
Hub diameter (m)	5.6
Gearbox ratio (-)	50
Shaft tilt angle (degrees)	5.0
Rotor pre-cone angle (degrees)	-2.5
Rotor mass (kg)	227,962
Nacelle mass (kg)	446,036
Hub height (m)	119.0
Tower length (m)	106.53
Distance from the transition piece to mean sea level (m)	10.0
Tower-top diameter (m)	7
Tower-base diameter (m)	10.5
Tower-top thickness (mm)	30
Tower-base thickness (mm)	57

3. MODAL ANALYSIS

3.1 FAST DESCRIPTION

The computational tool FAST developed by National Renewable Energy Laboratory (NREL) is used to perform the coupled analysis. The FAST tool consists of five major modules: AeroDyn, HydroDyn, ServoDyn, ElastDyn and SubDyn, as presented in Figure 2. The AeroDyn module employs the dynamic wake model and blade element momentum theory for the aerodynamic loads prediction. The Beddoes-Leishman dynamic stall model has been applied for the correction of the unsteady aerodynamic performance. In HydroDyn, the wave velocity and acceleration histories are generated using Airy wave theory based on a prescribed wave spectrum. Morison's equations are used to obtain the viscous drag of the support structure. Furthermore, the 2nd order wave kinematics are also examined. The pitch angle of each blade and rotational speed of the generator are controlled in the SeroDyn module through a dynamic link library (DLL) or an interface with MATLAB. In ElastDyn module, the dynamic responses of the tower and blades are calculated using linear modal approach. The SubDyn module is developed for structural dynamic analysis of bottom-fixed support structures. The support structure is modelled as a multi-member system. Each member is treated as

a two-node Timoshenko beam. The Craig-Bampton method is used for reducing the number of modes to obtain an accurate solution efficiently.

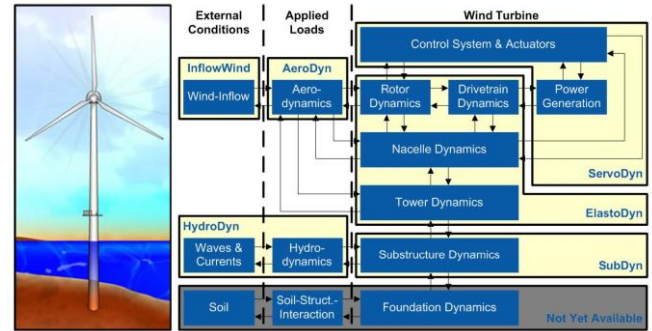


Figure 2: FAST control volumes for fixed-bottom systems [18]

3.2 MODAL RESULTS

The eigen-analysis is performed for the two wind turbine models using FAST and a finite element software suite, ABAQUS. Table 2 compares the eigen-frequencies of first two eigenmodes of the support structures in fore-aft (F-A) and side-side (S-S) directions. As presented in Table 2, the natural frequency corresponding to each eigenmode of the monopile wind turbine is lower than that of the tripod type. The results obtained using FAST agree well with those predicted by ABAQUS, indicating that the FAST can be used to examine the structural dynamic responses for the offshore wind turbine with a monopile or tripod. The modal shapes of the eigenmodes of the two wind turbines are presented in Figure 3.

Table 2: Eigen-frequencies of the two wind turbines obtained using FAST and ABAQUS (unit: Hz)

	Monopile		Tripod	
	FAST	ABAQUS	FAST	ABAQUS
1 st F-A	0.312	0.321	0.414	0.428
1 st S-S	0.312	0.320	0.412	0.421
2 nd F-A	1.669	1.715	2.537	2.727
2 nd S-S	1.668	1.706	2.247	2.403

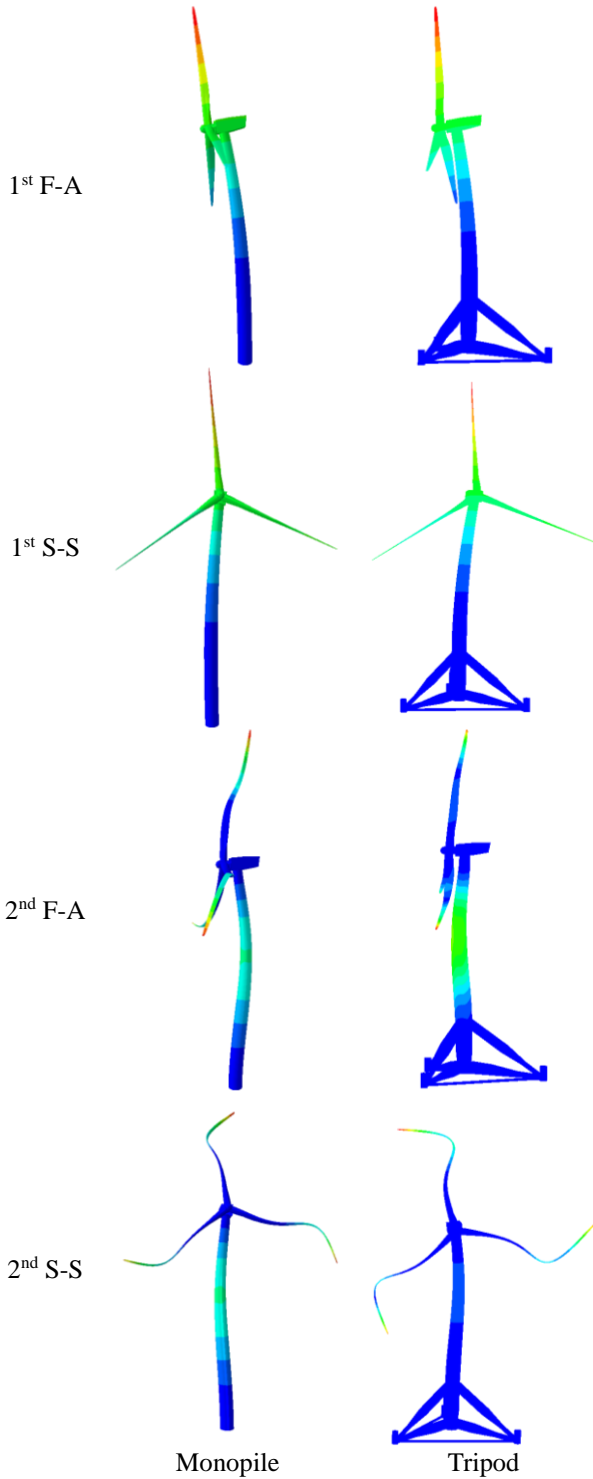


Figure 3: Modal shapes of the wind turbines

4. RESULTS AND DISCUSSIONS

4.1 WIND AND WAVE CONDITIONS

In order to generate a full-field turbulent wind for the analysis, the numerical program developed by NREL, TurbSim [19], is used. The wind field is discretized in finite grid points in vertical and horizontal directions by taking the hub as the

centre. To cover the operating domain of the wind turbine, a $200\text{m} \times 220\text{m}$ area is produced as shown in Figure 4. The velocity component in the x direction is perpendicular to the rotor plane while the directions of the other two components are also depicted in Figure 4.

Wind velocity of each grid point consists of a constant mean value \bar{V} and a turbulent component $V'(t)$. In this study, the mean velocity $\bar{V}(h)$ at height h is obtained using the power law profile with an exponent of 0.2:

$$\bar{V}(h) = V_{\text{hub}} \left(\frac{h}{H_{\text{hub}}} \right)^{0.2} \quad (1)$$

where V_{hub} is the mean velocity at the hub height H_{hub} . The value of V_{hub} is selected as 11.4 m/s equal to the rated wind speed.

The turbulent component $V'(t)$ is estimated by applying an inverse Fourier transformation to the IEC Kaimal turbulent spectrum described by [19]:

$$S_{\gamma}(f) = \frac{4\sigma_{\gamma}^2 L_{\gamma} V^{-1}}{(1 + 6fL_{\gamma}V^{-1})^{5/3}} \quad \gamma = x, y, z \quad (2)$$

where f is the frequency, V is the mean wind speed at hub height, σ_{γ} is the standard deviation of the wind speed and L_{γ} is the integral scale parameter of each velocity component.

The turbulence intensity is selected as level A (19.86% at hub). In accordance with IEC-64000-1, the standard deviations of the wind speed are 2.2 m/s, 1.76 m/s and 1.1 m/s for x , y and z directions, respectively. The values of L_{γ} equal to 486 m, 162 m and 39.6 m for x , y and z directions, respectively. Figure 5 presents the wind speed variations in the three directions at the hub height.

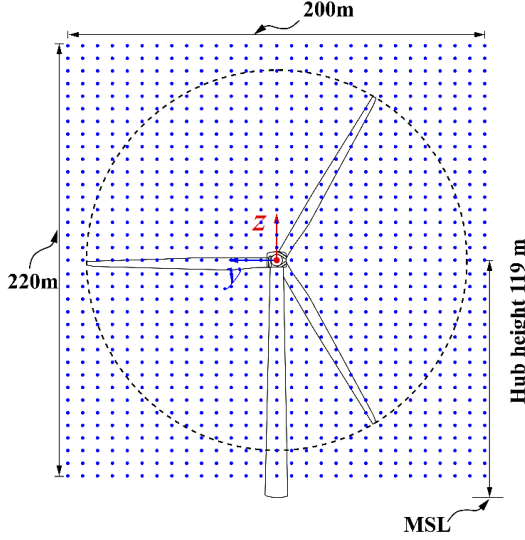


Figure 4: Grid discretization of wind filed domain

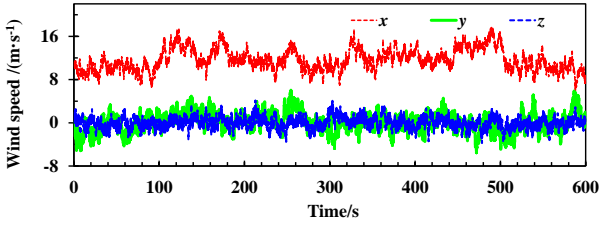


Figure 5: Wind speed at the hub height

The JONSWAP spectrum as denoted in Eq. (3) is used to generate the wave time histories.

$$S_{\zeta}(\omega) = 0.3125 H_s^2 T_p \left(\frac{\omega}{\omega_p} \right)^5 \exp \left[-\frac{5}{4} \left(\frac{\omega}{\omega_p} \right)^4 \right] \cdot (1 - 0.287 \ln \chi) \chi \exp \left[-\frac{(\omega - \omega_p)^2}{2\sigma^2 \omega_p^2} \right] \quad (3)$$

where H_s is the significant wave height and T_p is the wave period. The adopted values of H_s and T_p are 6 m and 9.9 s, respectively. $\omega_p = 2\pi/T_p$, $\sigma = 0.07$ for $\omega \leq \omega_p$ and $\sigma = 0.09$ for $\omega > \omega_p$. χ represents the JONSWAP peakedness parameter selected in terms of:

$$\chi = \begin{cases} 5 & T_p / \sqrt{H_s} \leq 3.6 \\ \exp(5.75 - 1.15 T_p / \sqrt{H_s}) & 3.6 < T_p / \sqrt{H_s} \leq 5 \\ 1 & T_p / \sqrt{H_s} > 5 \end{cases} \quad (4)$$

According to Airy theory, the wave time histories can be written as:

$$\eta(t) = \sum_{j=1}^N A_j \sin(\omega_j \cdot t - k_j \cdot \chi + \psi_j) \quad (5)$$

$$A_j = \sqrt{2S_{\zeta}(\omega_j) \Delta\omega} \quad (6)$$

$$V(z, t) = \sum_{j=1}^N \omega_j A_j \frac{\cosh[k(z + d_w)]}{T_p \sinh(kd_w)} \sin(\omega_j t - k_j \chi + \psi_j) \quad (7)$$

$$\mathcal{W}(z, t) = \sum_{j=1}^N \omega_j^2 A_j \frac{\cosh[k(z + d_w)]}{T_p \sinh(kd_w)} \cos(\omega_j t - k_j \chi + \psi_j) \quad (8)$$

where $\eta(t)$ is the wave elevation time history. ω is the wave frequency in rad/s. ψ_j is a random phase angle falling within 0 to 2π . d_w is the water depth, *i.e.* the distance between the mudline and MSL. z is the local water depth. k is the wave number related with z and ω as expressed in Eq. (9).

$$k \tanh(kz) = \omega^2 / g \quad (9)$$

where g is the gravitational acceleration.

For a specified water depth z , the wave number can be obtained by solving Eq. (9) to calculate the wave time histories. Figure 6 presents the wave elevation variation.

The current velocity at the local water depth z is calculated using a power law.

$$V_c(z) = V_0 \left(\frac{z + h}{h} \right)^{1/7} \quad (10)$$

where V_0 is the current velocity at MSL. The adopted value in this research is 0.55 m/s.

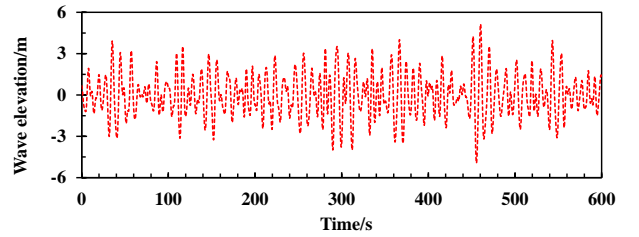


Figure 6: Wave elevation history

4.2 COUPLED DYNAMICS

The coupled dynamics of the monopile and tripod offshore wind turbines are examined using the FAST tool. The duration of the simulation is 600s and a start-up process is considered. The rotor thrust and the servo variables (rotor speed, blade pitch and generator power) are presented in Figure 7. The rotor thrust of the tripod fluctuates in the range of 0.52 MN to 2.24 MN, while the variation of the monopile in terms of the rotor thrust is 0.81 MN to 2.02 MN. The variation range of the monopile is slightly smaller compared to the

tripod. For both types of wind turbines, the rotor speed fluctuates around the rated value (9.6 rpm). The maximum rotor speed is 11.1 rpm for the monopile wind turbine, and corresponding value for the tripod type is 12.0 rpm. The minimum rotor speeds are 7.41 rpm and 6.69 rpm for the monopile and tripod respectively. It is noted that the rotor speed of the monopile wind turbine is closer to the rated rotor speed than that of the tripod type. The monopile wind turbine has a maximum pitch angle of 11.3 degrees, while the value is 12.0 degrees for the tripod. Regarding the generator power, several significant peaks deviated to the rated level, which can be observed from the results of the both wind turbines. However, the deviation corresponding to the monopile wind turbine is smaller than that of the tripod type. The presented results indicate that the monopile wind turbine operates more stably compared to the tripod type. A plausible reason for this is that the natural frequencies corresponding to the 1st fore-aft and side-side eigenmodes of the tripod support structure fall within the blade pass frequency range (3P, 0.3Hz ~ 4.8 Hz). This means the eigenmodes of the tripod support structure are more likely to be activated compared to the monopile type.

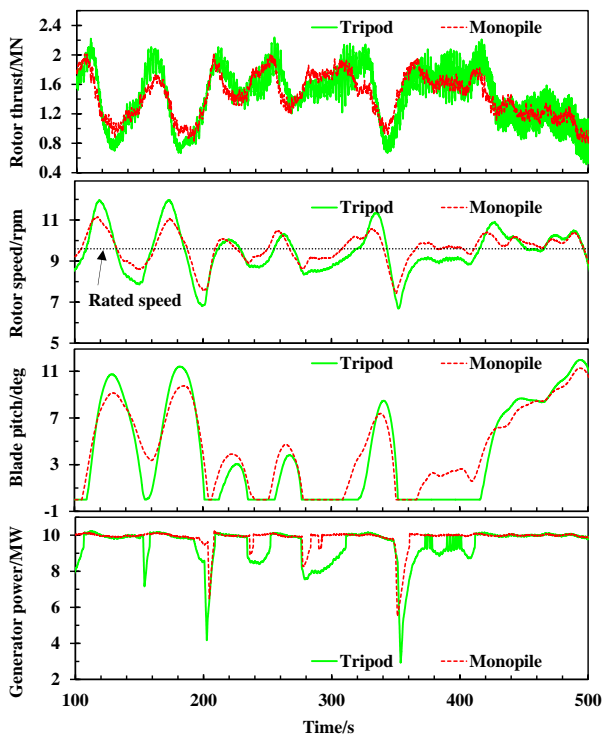


Figure 7: Comparisons for the rotor thrust and control variables

Figure 8 presents the blade-tip deflections of the two wind turbine models. For the monopile wind

turbine, the out-of-plane blade-tip deflection varies from 1.37m to 10.16m with an average value of 6.44m. Meanwhile, the tripod type has a fluctuation range of 1.28m to 10.98m with an average value of 6.53m in terms of the out-of-plane blade-tip deflection. Regarding the in-plane results, the difference between the two turbines is insignificant compared to the out-of-plane results.

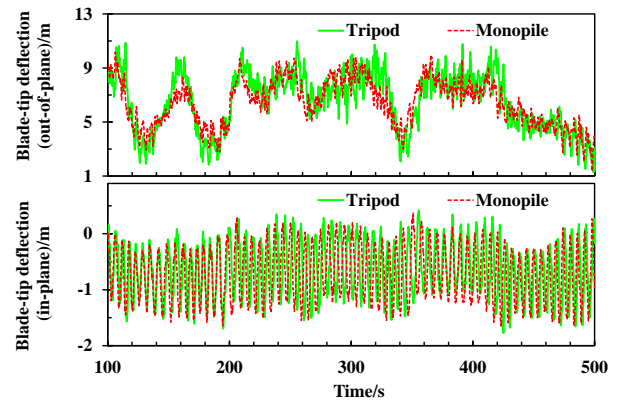


Figure 8: The blade-tip deflections

The frequency domain results associated with the blade-tip deflections are presented in Figure 9. The values at 0 Hz of the out-of-plane deflection corresponding to the monopile and tripod are 12.6m and 12.8m, respectively. The amplitudes at the rotational frequency (1P, 0.16 Hz) are 0.20m and 0.18m for monopile and tripod, respectively. That means the elastic deformation dominates the out-of-plane deflection at the blade-tip. It is also noted that the amplitude at the 1P frequency of the tripod wind turbine is slightly larger than that of the monopile type. For the both wind turbines, the flapwise mode of the blade has insignificant contribution to the out-of-plane vibration since no peak was observed at the corresponding eigen-frequency (0.63 Hz). Meanwhile, significant amplitudes are observed at the 1st edgewise mode of the blade in terms of the in-plane deflection for the two wind turbines. The tripod type has a larger peak at the corresponding eigen-frequency compared to the monopile wind turbine.

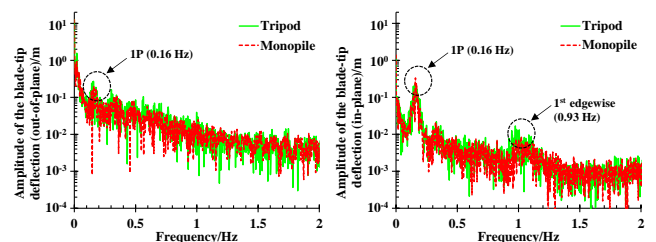


Figure 9: Frequency domain results of the blade-tip deflections

5. CONCLUSIONS

This study compares the dynamic responses of a monopile structure and a tripod one for a 10 MW wind turbine. The baseline tower which was designed for a land-based wind turbine has been scaled up in order to satisfy the structural strength requirements for the application in 50m water depth. Fully coupled time domain simulations are carried out using an open source tool, FAST. The modal analysis of the two wind turbines are performed in FAST and ABAQUS. The eigenfrequency of each mode is predicted using FAST agrees well with that obtained by ABAQUS. It is noted the tripod wind turbine has a higher eigenfrequency for each mode of the support structure. The comparisons of the time domain results indicate the monopile wind turbine operates in a more stable manner compared to the tripod wind turbine. The eigenmodes of the tripod support structure are more likely to be activated compared to the monopile type, since the natural frequencies corresponding to the 1st fore-aft and side-side eigenmodes of the tripod support structure fall within the 3P frequency range. The fluctuation range of the controller variables of the monopile wind turbine is smaller than that of the tripod type, resulting in smaller blade-tip deflections. The frequency domain results indicate that the 1P frequency has significant contribution to the blade-tip deflections at both flapwise and edgewise. The activation of the 1st edgewise mode has been confirmed by the observation of the significant peak at the corresponding frequency (0.93 Hz), while the contribution of the 1st flapwise mode is invisible. The results presented in this study contributes to the improvements in the design of support structures of large wind turbines.

ACKNOWLEDGEMENTS

The authors would like to acknowledge the financial supports from the National Natural Science Foundation of China (grant numbers: 51676131 and 51811530315) and the Royal Society (grant number: IEC\NSFC\170054). The first author and the last author are particularly grateful to the Chinese Scholarship Council for funding their overseas studies in the UK.

REFERENCES

1. GLOBAL WIND ENERGY COUNCIL, 2018 'Global Wind Report: Annual Market Update 2017', *GWEC report*.
2. EUROPEAN WIND ENERGY ASSOCIATION, 2014 'The European Offshore Wind Industry—Key Trends and Statistics 2013', *EWEA report*.
3. C. BAK, R. BITSCHKE, A. YDE, et al. 2012 'Light Rotor: The 10-MW Reference Wind Turbine', *Proceedings of the European Wind Energy Association (EWEA) Annual Event, Copenhagen*, pp. 16-19.
4. J. VELARDE, 2016 'Design of Monopile Foundations to Support the DTU 10 MW Offshore Wind Turbine', *Master thesis, Norwegian University of Science and Technology*.
5. J. VELARDE, E.E. BACHYNSKI, 2017 'Design and Fatigue Analysis of Monopile Foundations to Support the DTU 10 MW Offshore Wind Turbine', *Energy Procedia*, 137, pp.3-13.
6. AMERICAN PETROLEUM INSTITUTE, 2003 'Recommended Practice for Planning, Designing and Constructing Fixed Offshore Platforms—Working Stress Design'. *API Publishing Services: Washington, D.C.*
7. S. BISOI, S. HALDAR, 2014 'Dynamic Analysis of Offshore Wind Turbine in Clay Considering Soil–Monopile–Tower Interaction', *Soil Dynamics and Earthquake Engineering*, 63, pp.19-35.
8. R. SHIRZADEH, C. DEVRIENDT, M.A. BIDAQHVIDI, et al, 2013 'Experimental and Computational damping Estimation of an Offshore Wind Turbine on a Monopile foundation', *Journal of Wind Engineering and Industrial Aerodynamics*, 120, pp.96-106.
9. E. LOZANO, A.J. KOLIOS, F.P. BRENNAN, 2011, 'Multi-Criteria Assessment of Offshore Wind Turbine Support Structures', *Renewable Energy*, 36(11), pp.2831-2837.
10. A. BANERJEE, T. CHAKRABORTY, V. MATSAGAR, 2018 'Evaluation of Possibilities in Geothermal Energy Extraction from Oceanic Crust Using Offshore Wind Turbine Monopiles', *Renewable and Sustainable Energy Reviews*, 92, pp.685-700.
11. S. AASEN, A.M. PAGE, K.S. SKAU, et al,

- 2017 'Effect of Foundation Modelling on the Fatigue Lifetime of a Monopile-Based Offshore Wind Turbine', *Wind Energy Science*, 2, pp. 361-376.
12. W. CARSWELL, S.R. ARWADE, D.J. DEGROOT, et al, 2015 'Soil-Structure Reliability of Offshore Wind Turbine Monopile Foundations', *Wind Energy*, 18(3), pp.483-498.
 13. M. ARSHAD, B.C. KELLY, 2013 'Offshore Wind-Turbine Structures: a Review', *Proceedings of the Institution of Civil Engineers-Energy*, 166(4), pp.139-152.
 14. A. MORATÓ, S. SRIRAMULA, N. KRISHNAN, 2017 'Ultimate Loads and Response Analysis of a Monopile Supported Offshore Wind Turbine Using Fully Coupled Simulation', *Renewable Energy*, 101, pp.126-143.
 15. K.A. ABHINAV, N. SAHA, 2018 'Nonlinear Dynamical Behaviour of Jacket Supported Offshore Wind Turbines in Loose Sand', *Marine Structures*, 57, pp.133-151.
 16. J. JONKMAN, W. MUSIAL, 2010 'Offshore Code Comparison Collaboration (OC3) for IEA Wind Task 23 Offshore Wind Technology and deployment', *National Renewable Energy Laboratory, Technical Report No. NREL/TP-5000-48191*.
 17. H. SONG, R. DAMIANI, A. ROBERTSON, et al, 2013 'A New Structural-Dynamics Module for Offshore Multimember Substructures Within the Wind Turbine Computer-Aided Engineering Tool FAST' *The 23rd International Offshore and Polar Engineering Conference, International Society of Offshore and Polar Engineers*.
 18. B. JONKMAN, J. JONKMAN, 2016 'FAST v8. 16.00 a-bjj'. *National Renewable Energy Laboratory*.
 19. B. JONKMAN, 2009 'TurbSim User's Guide: Version 1.50'. *National Renewable Energy Laboratory, Technical Report No. NREL/TP-500-46198*.